

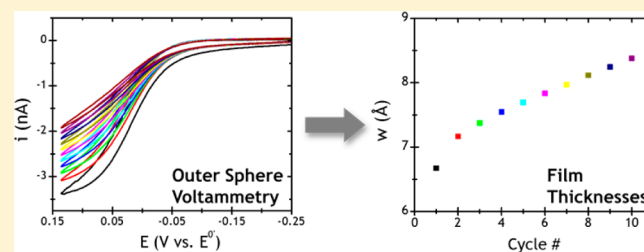
# Electrochemical Nonadiabatic Electron Transfer via Tunneling to Solution Species through Thin Insulating Films

Caleb M. Hill,<sup>§</sup> Jiyeon Kim, Nataraju Bodappa, and Allen J. Bard<sup>\*,†</sup>

University of Texas at Austin, Austin, Texas 78705, United States

**S** Supporting Information

**ABSTRACT:** Described here is a semiquantitative theoretical treatment of the kinetics of outer sphere electrochemical reactions. The framework presented here, which is based on simple physical arguments, predicts heterogeneous rate constants consistent with previous experimental observations ( $k^0 > 10$  cm/s). This theory is applied to the analysis of voltammetry experiments involving ultramicroelectrodes modified with thin, insulating oxide films where electronic tunneling between the electrode and redox species in solution (metal–insulator–solution tunneling) is expected to play a prominent role. It is shown that analysis of the voltammetric response of an outer sphere redox couple can be used to track changes in the structure of the adsorbed insulating layer.



## INTRODUCTION

The kinetics of electron transfer between a metal electrode and a redox species which has been spatially separated from said electrode by means of an insulating film is a topic of fundamental importance in many electrochemical systems. Such systems are unique in that the heterogeneous electrochemical reaction rate is significantly impacted by the electronic coupling between the electrode and the redox species, the so-called “nonadiabatic” kinetic regime. Here, we describe a theoretical model for the heterogeneous electron transfer kinetics in these systems which predicts their behavior based on the properties of the insulating film and the concentration of redox species in solution.

The most frequent examples of electrochemical systems which exhibit nonadiabatic electron transfer kinetics employ electrodes (usually Au) covered by organic self-assembled monolayers (SAMs). Initial studies into nonadiabatic electron transfer in these systems involved redox species freely diffusing in solution,<sup>1,2</sup> which presented problems due to the near universal presence of pinholes in alkane-thiol SAMs. This issue was largely circumvented by the covalent attachment of redox moieties to the SAM itself, and most subsequent studies of nonadiabatic electrochemical kinetics have followed this concept.<sup>3–8</sup> Theoretical treatments for this situation, where the redox active species is held at a well-defined distance and orientation with respect to an electrode, have been reported previously by Gosavi and Marcus.<sup>9,10</sup> Thin (ca. 1 nm) semiconducting films, such as TiO<sub>2</sub>, have been recently explored as alternative insulating films for studies at passivated electrodes.<sup>11–15</sup> These films do not appear to suffer from the same problems with regards to pinholes and leakage as organic SAMs, and may allow for more rigorous investigations into the

kinetics of electron transfer through an insulating film to redox species diffusing freely in solution.

In addition to fundamental studies of electron transfer kinetics, such ultrathin inorganic insulating films are promising as a method of electrode modification for advanced electroanalytical and electrocatalytic studies (providing a novel platform to study electrochemistry at individual nanostructures<sup>11,13</sup>) and as protecting layers against corrosion in photoelectrochemical cells.<sup>16–18</sup> For applications such as these, it would be advantageous to have a simple, electrochemical means of characterizing ultrathin inorganic films (e.g., voltammetry using common outer sphere redox molecules), which requires a working theoretical treatment of the electrode kinetics in these systems.

We have recently reported a theoretical treatment of kinetics for the “tunneling ultramicroelectrode”, where a conventional ultramicroelectrode (UME) is passivated by a thin semiconducting layer and a metal nanoparticle (NP) is attached to the surface of the passivated electrode, effectively reestablishing electrical contact with an electrolyte solution via tunneling between the NP and the underlying electrode.<sup>12</sup> In this treatment, the overall electrochemical process was treated as a consecutive, two-step reaction, with electron tunneling from the electrode to the adsorbed NP followed by heterogeneous electron transfer to a redox species in solution. Here, we extend parts of this basic approach to the more general case of direct electron transfer between a passivated electrode and redox species diffusing freely in solution. This report gives a semiquantitative theoretical treatment of this case, along with applications to relevant experimental data. The primary

Received: December 2, 2016

Published: April 9, 2017

question we seek to answer through the application of this model is can simple, outer sphere electrode voltammetry be employed to characterize thin insulating films applied to electrodes?

## RESULTS AND DISCUSSION

**Basics of the Present Model.** To preserve readability, the theoretical treatment will only be roughly outlined here. Detailed derivations and a complete glossary of mathematical symbols are provided in the [Supporting Information](#) (SI). For the outer sphere reduction,  $O + e^- \rightleftharpoons R$ , where O and R are diffusing freely in solution, the following form for the forward rate,  $k_f$ , is commonly cited:<sup>19–21</sup>

$$k_f(E) = Z \exp\left\{-\frac{(\lambda + q(E - E^0))^2}{4\lambda kT}\right\}$$

$$Z = \sqrt{\frac{kT}{2\pi m_O}} \quad (1)$$

where  $\lambda$  is the reorganization energy (for which we will only consider outer-sphere contributions),  $kT$  is Boltzmann's constant times temperature,  $q$  is the charge of 1 electron,  $E$  the applied potential,  $E^0$  the formal potential for the reaction, and  $m_O$  is the mass of O/R.  $Z$  represents the expected gas-phase collision rate of O with the electrode surface. Here, we will employ an approach similar to that originally proposed by Feldberg<sup>22</sup> where the heterogeneous electron transfer constant  $k_f$  contains contributions from species at varying distances from the electrode surface:

$$k_f(E) = \int_{z_0}^{\infty} k_1(z, E)\gamma(z, E) dz \quad (2)$$

Here,  $k_1$  is the “adiabatic” rate (in  $s^{-1}$ ) and  $\gamma$  is a tunneling factor which accounts for the probability of electron transfer from the electrode through any insulating layers to the reorganized complex  $O^\ddagger$  in solution. Both factors will vary with  $z$ , the distance from the electrode surface, and  $z_0$  is the distance of closest approach for the redox species in solution.  $\gamma$  will depend on the electronic properties of the electrode and insulating layers (see [SI](#) for derivation):

$$\gamma(z, E) = \frac{k_2(z, E)}{2k_2(z, E) + k_{-1}}$$

$$\frac{k_2}{k_{-1}} = \frac{S\sigma}{(w+z)^2} [1 + \beta(z, E)] e^{-\beta(z, E)}$$

$$\beta(z, E) = 2a(w+z)\bar{\varphi}^{1/2}(z, E)$$

$$S = \frac{\pi\hbar\rho_F}{a^2 m_e v_F} \quad (3)$$

where  $k_2$  is the tunneling rate,  $\sigma$  is an effective cross-section for the redox molecule,  $\hbar$  is Planck's constant ( $h$ ) divided by  $2\pi$ ,  $m_e$  is the electron mass,  $\rho_F$  is the Fermi-level density of states for the metal electrode,  $v_F$  is the Fermi velocity,  $a$  is a constant equal to  $0.512 \text{ eV}^{-1/2} \text{ \AA}^{-1}$ ,  $w$  is the thickness of an insulating layer on the electrode surface, and  $\bar{\varphi}^{1/2}(z, aE)$  is the average tunneling barrier height.

After considering electron transfer from all possible metal states, the overall forward rate constant,  $k_f$ , can be expressed as follows:

$$k_f(E) = \frac{kT}{h} \left[ \frac{1}{2} \operatorname{erfc}\left\{ \frac{\lambda + q(E - E^0)}{\sqrt{4\lambda kT}} \right\} \right] \Gamma(E)$$

$$\Gamma(E) = \int_{z_0}^{\infty} \gamma(z, E) dz \quad (4)$$

Here,  $\Gamma$  represents the effective distance into solution with which the electrode can interact with redox species and is the only term dependent on the thickness of the insulating layer.  $\Gamma$  will vary with the applied electrode potential and the electronic properties of the solvent and any insulating layers on the electrode.

**Equivalent Butler–Volmer Expressions.** It will be convenient to compare the expression for  $k_f$  derived here to the classical Butler–Volmer expression for electrode kinetics:

$$k_{f,BV} = k^0 e^{-\alpha q(E - E^0)/kT} \quad (5)$$

where  $\alpha$  is a constant which can vary between 0 and 1, but is found to be around 0.5 for many electrochemical systems. For small values of  $E - E^0$ , the present form for  $k_f$  can be shown to agree with the Butler–Volmer expression:

$$k_{f,BV} \approx \frac{(kT)^{3/2}}{h(\pi\lambda)^{1/2}} \Gamma(E) \exp\left[-\frac{\lambda + 2q(E - E^0)}{4kT}\right]$$

$$k_{BV}^0 = \frac{(kT)^{3/2}}{h(\pi\lambda)^{1/2}} \Gamma^0 \exp\left[-\frac{\lambda}{4kT}\right]$$

$$\alpha_{BV} = \frac{1}{2} + \frac{q(E - E^0)}{2\lambda} - \frac{kT}{q\Gamma(E)} \frac{\partial\Gamma(E)}{\partial E} \quad (6)$$

where  $\Gamma^0 = \Gamma(E = E^0)$ . The most interesting result here is the expression for the transfer coefficient,  $\alpha$ . The first two terms in this expression represent the classical result of Marcus theory, which predicts  $\alpha$  is 0.5 at  $E = E^0$  but also varies linearly with the applied potential. The third term in the expression, which is unique to the present treatment, accounts for potential dependent changes in the value of  $\Gamma$ . This provides an additional mechanism for a potential dependence of  $\alpha$ ,<sup>23–27</sup>

one which allows for a deviation from 0.5 at  $E = E^0$ . Such a deviation at  $E = E^0$  is not accounted for in the standard Marcus-type treatment of electrode kinetics, although it has also been shown to result from an “asymmetric” version of Marcus theory,<sup>28</sup> where the force constants for the reactant and product surfaces are taken to be inequivalent.

**Basic Ramifications of the Present Theory.** Simulated cyclic voltammograms employing the described kinetic model are given in [Figure 1](#) for a reduction. For this system, with an offset of 1 eV between the Fermi level of the metal and the conduction band edge of the insulating layer, significant changes are seen in the voltammetric response at film thicknesses as small as 4 to 6 Å. The voltammograms are gradually shifted to more negative potentials with increasing film thickness. The change in  $k^0$  for the system as a function of  $w$  is given in the inset. As is typical in systems involving tunneling through an insulating film,  $k^0$  decreases exponentially with  $w$  from an initial value of ca. 7 cm/s for  $w = 0$  (i.e., a bare electrode). From the data in the inset, an effective barrier height of  $\sim 0.5$  eV can be roughly estimated using the slope of  $\ln k^0$  vs  $w$  ( $\sim 0.7 \text{ \AA}^{-1}$ ). This value is lower than the 1 eV offset

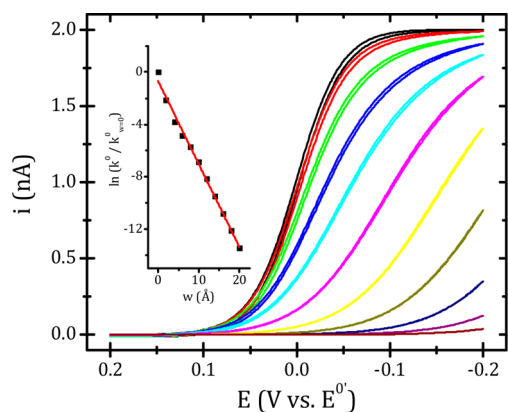


**Figure 1.** Simulated cyclic voltammograms for the reduction of a hypothetical system with parameters given in Table 1 and film thicknesses,  $w$ , varying between 0 and 20 Å in 2 Å increments. The inset shows the evolution of  $k^0$  given as a plot of  $\ln(k^0/k_{w=0}^0)$  vs  $w$ , where  $k_{w=0}^0$  is the value of  $k^0$  with no film present. Simulations were carried out for a bulk concentration of 1 mM, an electrode diameter of 10  $\mu\text{m}$ , and a diffusion constant of  $10^{-5}$   $\text{cm}^2/\text{s}$ .

mentioned above due to the lowering of the effective barrier by image charge effects (see SI). It is encouraging that these numbers correlate favorably with experiments concerning the kinetics of fast outer-sphere redox couples, but these values should be treated with caution due to the many underlying assumptions made in the estimation of absolute reaction rates as well as the numerous physical parameters involved in the calculations (see Table 1).

**Table 1. Values for Various Parameters Used in the Calculations in This Report<sup>a</sup>**

	Figure 1	Ta/Ta <sub>2</sub> O <sub>5</sub>	Pt/TiO <sub>2</sub>
$\Phi_M$ (eV)	5.4	4.2 <sup>40</sup>	5.6 <sup>40</sup>
$V_I$ (eV)	-4.4	-3.5 <sup>41</sup>	-4.2 <sup>42</sup>
$V_S$ (eV)	-1.2	-1.0 <sup>b</sup>	-1.2 <sup>43</sup>
$\rho_F(10^{22}$ eV/cm <sup>3</sup> )	1.7	7 <sup>44</sup>	15 <sup>44</sup>
$\nu_F(10^7$ cm/s)	13	6.5 <sup>44</sup>	4.4 <sup>44</sup>
$n_S^2$	1.8	2.1 <sup>40</sup>	1.8 <sup>40</sup>
$\epsilon_S$	80	10 <sup>40</sup>	80 <sup>40</sup>
$n_I^2$	5	4.5 <sup>45</sup>	6.4 <sup>40</sup>
$\epsilon_I$	20	25 <sup>46</sup>	31 <sup>47</sup>
$E^{0'}$ (eV)	-4.5	-5.1 <sup>c</sup>	-4.9 <sup>40</sup>
$r_o$ (Å)	4	3.5 <sup>48</sup>	3.5 <sup>48</sup>
$\Gamma^0$ (Å)	0.1	0.3	1.1
$k_{BV}^0$ (cm/s)	7	70	40
$\alpha_{BV}^0$	0.51	0.52	0.51

<sup>a</sup> $\Phi_M$  is the work function of the metal electrode.  $V_I$  and  $V_S$  are the conduction band edges of the insulator and the solvent and are referenced vs. vacuum level, as is the formal reduction potential,  $E^{0'}$ . <sup>b</sup>Estimated value. <sup>c</sup>Calculated by applying difference between Born solvation energies in H<sub>2</sub>O and DCE.

## APPLICATION TO EXPERIMENT

To illustrate the applications of the proposed model, experiments were undertaken with two tunneling layers: Ta<sub>2</sub>O<sub>5</sub>, formed by air oxidation of Ta, and TiO<sub>2</sub>, formed by electrochemical oxidation of Ti(III) on Pt. The thickness of the layers was found from the measured electrode capacitance and

the dielectric constants shown in Table 1. Experimental details are given below.

**Ta<sub>2</sub>O<sub>5</sub>.** In order to provide a test of the model presented here, the voltammetry of an outer sphere redox couple, ferrocene methanol (FcMeOH), at Ta/Ta<sub>2</sub>O<sub>5</sub> UMEs was investigated. Ta surfaces spontaneously form thin (ca. 2.5 nm), insulating native oxide films upon exposure to oxygen.<sup>29</sup> Cyclic voltammetry (CV) was used to changes in electrode activity under conditions in which the growth of such a native oxide film is reasonably slow (anhydrous organic media in an Ar-filled glovebox). The general scheme is depicted in Figure 2. In an

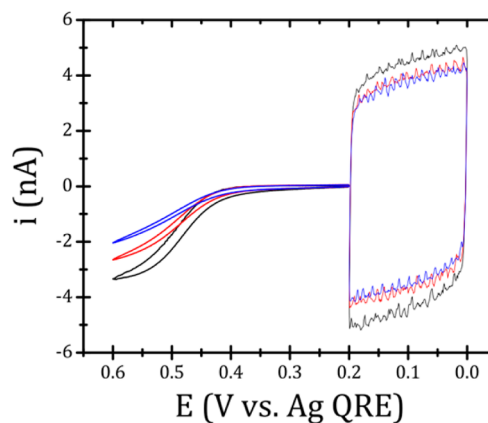


**Figure 2.** Voltammetry of a ca. 25  $\mu\text{m}$  diameter tantalum disk UME in 1 mM FcMeOH, 100 mM TBAPF<sub>6</sub> in DCE. Fast (50 V/s) CVs between 0.2 and 0 V are used to measure capacitance for estimating the thickness of the Ta<sub>2</sub>O<sub>5</sub> film, while slower (0.025 V/s) CVs are used to probe the reactivity of the UME toward FcMeOH oxidation. Different colors denote subsequent cycles.

alternating fashion, slow (25 mV/s) CV scans were employed to probe the kinetics of FcMeOH oxidation and fast (50 V/s) CV scans were obtained in a potential region where no faradaic reaction occurred to measure the differential capacitance of the electrode, which can be related straightforwardly to the thickness of the Ta<sub>2</sub>O<sub>5</sub> layer (see SI). Thus, these experiments provide a means of correlating gradual changes in the kinetic properties of the UME with increases in the thickness of the insulating layer.

CVs for FcMeOH oxidation at a Ta/Ta<sub>2</sub>O<sub>5</sub> UME through 11 cycles are given in the left panel of Figure 3. The initial scan (black curve) is close to that expected for a mass transfer controlled reaction. Measured currents at a given potential decrease in subsequent scans and the profile takes on that of a severely kinetically limited process, both of which would be expected for increasing thicknesses of the Ta<sub>2</sub>O<sub>5</sub> film. Note that the diffusion limited current should be the same at sufficiently positive potentials. These experimental CVs were fit to theoretical calculations according to the present kinetic model, using the Ta<sub>2</sub>O<sub>5</sub> film thickness,  $w$ , as the only variable parameter. The other relevant parameters (which were fixed during the fitting procedure) are given in Table 1. These fits are given in the right panel of Figure 3. The agreement with the experimental curves is reasonable, though not exact. A significant source of error here is the assumption that  $w$  is a constant within each cycle. In reality,  $w$  should be steadily increasing through the entire experiment, which would explain the “tailing off” of the current at higher potentials seen in the experiment which the present theory does not account for.

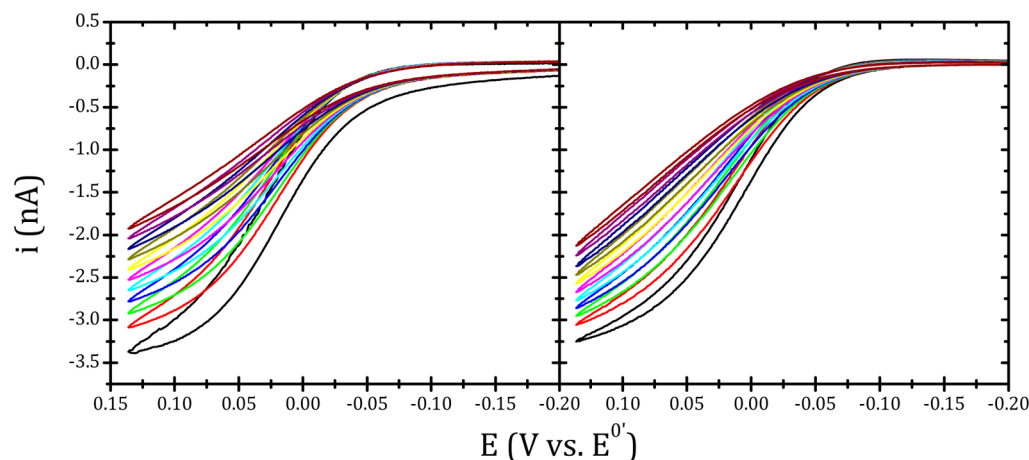


**Figure 3.** Voltammetry of a ca. 25  $\mu\text{m}$  diameter Ta UME in 1 mM FcMeOH, 100 mM TBAPF<sub>6</sub> in DCE. Different colors denote subsequent cycles. Experimental curves are given in the left panel, and theoretical curves obtained using the values given in Table 1 are given in the right panel.

The values for  $w$  derived from fitting the outer sphere voltammetry are found to be  $<10$  Å, which is reasonable for a film which permits tunneling to a significant degree. These film thicknesses were compared to thicknesses calculated from the differential capacitance of the electrode (see SI), a more conventional method of tracking changes in the structure of the electrode–electrolyte interface. The comparison between these values is given in Figure 4. The plot of values obtained via the

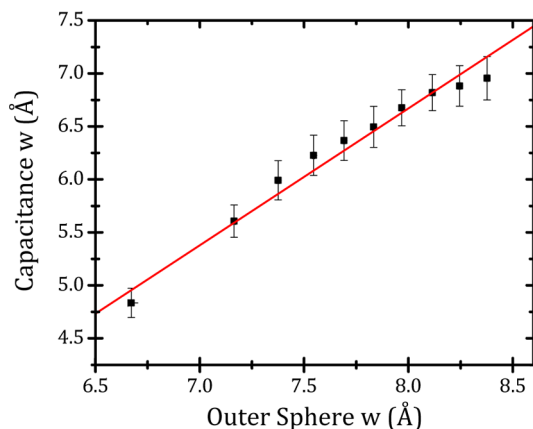


**Figure 4.** Plot of the Ta<sub>2</sub>O<sub>5</sub> film thickness,  $w$ , calculated from the measured electrode capacitance vs  $w$  obtained from fitting the outer sphere voltammetry given in Figure 3 to the present theoretical model.

two methods is linear within the experimental error, with a slope of ca. 1 and an absolute error of  $<2$  Å, lending validity to the present theoretical model.

**TiO<sub>2</sub>.** Another model system explored in these studies were electrodes composed of Pt, a common UME material, passivated by TiO<sub>2</sub> films. The TiO<sub>2</sub> films were deposited using an electrodeposition technique described previously.<sup>30,15</sup> In this way, very thin (ca. 1 nm) films can be produced with high repeatability and control. The effect of the thickness of the TiO<sub>2</sub> films on the outer sphere voltammetry of the Pt/TiO<sub>2</sub> UMEs was tested by cyclic voltammetry in between sequential deposition steps. The results of one such experiment are given in Figure 5.

When the present model is applied to the data in Figure 5 using the parameters given in Table 1, film thicknesses of ca. 6, 7.5, and 8.5 Å were obtained. This is consistent with previous

reports from this group concerning the thickness of TiO<sub>2</sub> films deposited using this technique.<sup>30,13</sup> Similarly to the Ta/Ta<sub>2</sub>O<sub>5</sub> case, the consistency between the present theory and previous experiments lend validity to the former, but the results should be treated with care due to the uncertainties introduced by the underlying assumptions of the model and possible errors in the parameters employed.

The effect of the concentration of redox species was also investigated experimentally using Pt/TiO<sub>2</sub> UMEs. According to the theory presented here, the heterogeneous rate constant does not depend on the concentration of redox species. That is, there is no “minimum” concentration of species in solution required for charge transfer across the insulating film. This stands in contrast to recent previous reports concerning the mediation of charge transfer across insulating films through the addition of metallic nanoparticles.<sup>30,12,31–39</sup> In the case involving metal nanoparticles, facile kinetics are restored by locally increasing the available electronic density of states at the surface of the insulating film, thus providing an intermediary for electron tunneling.

As expected, currents obtained at the Pt/TiO<sub>2</sub> UMEs show a linear dependence on the concentration of the redox species, which can be seen in Figure 6 for FcMeOH and Figure 7 for Fe(CN)<sub>6</sub><sup>3-</sup>. FcMeOH was investigated at concentrations up to 1 mM and several potentials. Fe(CN)<sub>6</sub><sup>3-</sup> was also investigated, due to the ability to investigate a wider concentration range. In both cases, linear behavior was observed, consistent with theoretical expectations.

## CONCLUSIONS

A semiquantitative framework for treating the rate of purely outer sphere heterogeneous electron transfer reactions was presented. The reported theory predicts rate constants for a commonly employed redox molecule, FcMeOH, consistent with experimental observations ( $k^0 > 10$  cm/s). This theory was applied to experiments involving voltammetry at electrodes modified by thin insulating layers (Ta/Ta<sub>2</sub>O<sub>5</sub> and Pt/TiO<sub>2</sub>). In both cases, it was demonstrated that the present theory allows one to correlate changes in outer sphere voltammetry to changes in the thickness of the insulating layer. It was also shown using Pt/TiO<sub>2</sub> electrodes that there was no unexpected concentration dependence in the behavior of tunneling in these metal–insulator–solution systems.

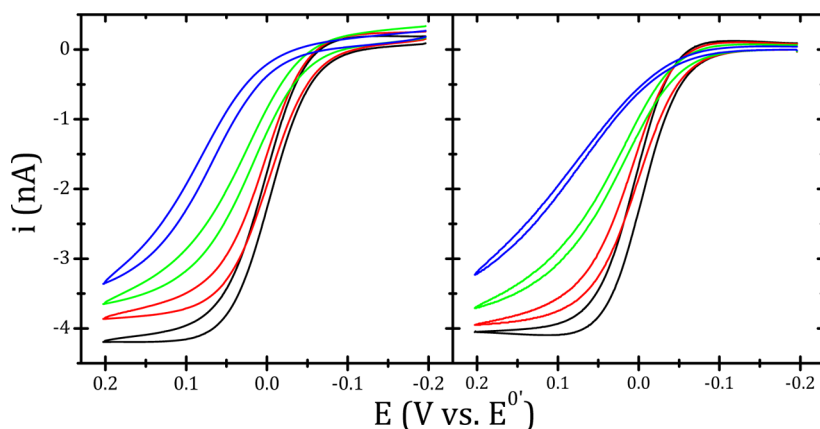


**Figure 5.** CVs of 1 mM FcMeOH, 10 mM KClO<sub>4</sub> at a 25  $\mu$ m diameter bare Pt UME (black line) and after several deposition steps (colored lines). Experimental curves are given in the left panel, and theoretical curves obtained using the values given in Table 1 are given in the right panel.

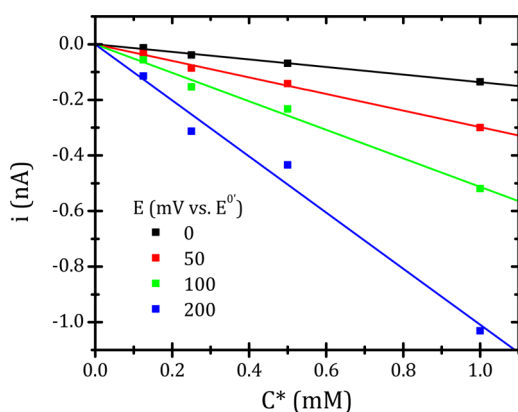


**Figure 6.** Steady state FcMeOH oxidation currents at a 25  $\mu$ m diameter Pt/TiO<sub>2</sub> UME held at various potentials in various concentrations ( $C^*$ ) of FcMeOH and 10 mM KClO<sub>4</sub>.

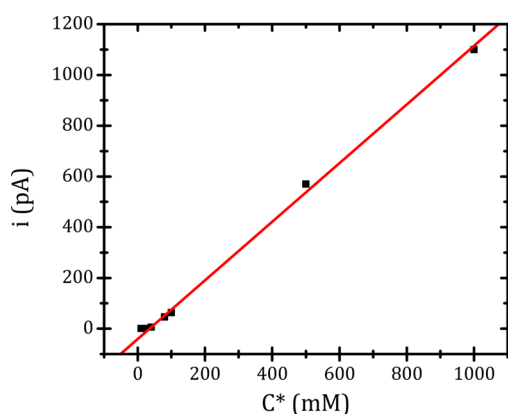


**Figure 7.** Steady state Fe(CN)<sub>6</sub><sup>3-</sup> reduction currents at a 200  $\mu$ m diameter Pt/TiO<sub>2</sub> UME held at 0 V vs Ag/AgCl in various concentrations ( $C^*$ ) of Fe(CN)<sub>6</sub><sup>3-</sup>.

## EXPERIMENTAL SECTION

**Fabrication of Ta/Ta<sub>2</sub>O<sub>5</sub> UMEs.** Glass capillaries (1.5 mm OD, 0.86 mm ID) were cleaned by brief (ca. 5 min) sonication in acetone, EtOH, and deionized (DI) H<sub>2</sub>O and dried in a 100 °C oven. One end of the capillaries was then sealed in a gas/oxygen flame. Ta wires (ca. 1 cm in length, 99% metals basis, Alfa Aesar) were loaded through the open end of the capillaries and brought to the sealed end by gently tapping the capillary on a lab bench. The wires were then sealed by heating the capillaries under vacuum using a nichrome coil. Electrical

leads were connected to the Ta wires using Ag epoxy (EPO-TEK H20E, Epoxy Technology), and the opening was sealed using quick-drying epoxy. The Ta wire was then exposed by sanding the tips of the capillaries on progressively finer grades of sandpaper. Final polishing was carried out on 3, 1, and 0.5  $\mu$ m diamond paper (3M).

**Voltammetry of Ferrocene at Ta/Ta<sub>2</sub>O<sub>5</sub> UMEs.** All electrochemical experiments employing Ta/Ta<sub>2</sub>O<sub>5</sub> electrodes were carried out in an Ar-filled glovebox (O<sub>2</sub> < 10 ppm, H<sub>2</sub>O < 0.1 ppm) to slow the formation of the insulating Ta<sub>2</sub>O<sub>5</sub> layer.

Ferrocene methanol (FcMeOH, 97%, Aldrich), tetrabutylammonium hexafluorophosphate (TBAPF<sub>6</sub>, 98%, Aldrich), and 1,2-dichloroethane (DCE, anhydrous, 98%, Sigma-Aldrich) were used as-received. Solids were dried overnight before being transferred into the glovebox, where all solutions were prepared.

Electrochemical measurements were carried out using a potentiostat (CHI 660D, CH Instruments) with Pt and Ag wires serving as counter and quasireference electrodes, respectively. Immediately prior to measurements, a Ta/Ta<sub>2</sub>O<sub>5</sub> UME was polished on a piece of dry 0.5  $\mu$ m diamond paper. The working electrode lead was then connected. A potential of 0.2 V vs Ag QRE was applied before the UME was introduced into solution. Cyclic voltammetry (CV) was then carried out, alternating between (1) 0.2 to 0 V to 0.2 V, 50 V/s, 10 cycles and (2) 0.2 to 0.6 V to 0.2 V, 0.025 V/s, 1 cycle. The “cell on” function of the CHI potentiostat was employed to ensure the working electrode potential was applied continuously throughout the measurements. The measurement process is depicted graphically in Figure 2.

**Pt/TiO<sub>2</sub> UMEs.** Pt UMEs were prepared in an analogous manner to the Ta UMEs described above, using 25  $\mu$ m Pt wire. TiO<sub>2</sub> films were prepared on the Pt UMEs according to a previously reported procedure.<sup>30,15</sup> Briefly, films were deposited onto Pt UMEs (cleaned by piranha solution) by the anodic hydrolysis of an aqueous solution of 50 mM TiCl<sub>3</sub> at a pH of 2.3. Each deposition cycle was carried out 20 mV positive of the open circuit potential for 5 s.

Between deposition cycles, the Pt/TiO<sub>2</sub> UME reactivity was checked via cyclic voltammetry in an aqueous solution of 1 mM FcMeOH, 10 mM KClO<sub>4</sub>. For all experiments with Pt/TiO<sub>2</sub> UMEs, Pt and Ag/AgCl (1 M KCl) served as counter and reference electrodes, respectively, unless otherwise noted.

## ASSOCIATED CONTENT

### Supporting Information

The Supporting Information is available free of charge on the ACS Publications website at DOI: 10.1021/jacs.6b12104.

Detailed derivations of the mathematical expressions and further discussion of the theoretical model (PDF)

## ■ AUTHOR INFORMATION

## Corresponding Author

\*ajbard@mail.utexas.edu

ORCID 

Allen J. Bard: 0000-0002-8517-0230

## Present Addresses

<sup>§</sup>Department of Chemistry, University of Wyoming, Laramie, WY 82071, United States<sup>†</sup>Department of Chemistry, Center for Electrochemistry, The University of Texas at Austin, Austin, TX 78712, United States.

## Notes

The authors declare no competing financial interest.

## ■ ACKNOWLEDGMENTS

C. M. H. would like to acknowledge J. E. Dick and C. Renault for helpful discussion. We acknowledge support of this research from the AFOSR MURI (FA9550-14-1-0003) and the Robert A. Welch Foundation (F-0021).

## ■ REFERENCES

- (1) Miller, C.; Cuendet, P.; Graetzel, M. *J. Phys. Chem.* **1991**, *95* (2), 877.
- (2) Porter, M. D.; Bright, T. B.; Allara, D. L.; Chidsey, C. E. D. *J. Am. Chem. Soc.* **1987**, *109* (12), 3559.
- (3) Chidsey, C. E. D. *Science* **1991**, *251*, 919.
- (4) Smalley, J. F.; Feldberg, S. W.; Chidsey, C. E. D.; Linford, M. R.; Newton, M. D.; Liu, Y.-P. *J. Phys. Chem.* **1995**, *99* (35), 13141.
- (5) Smalley, J. F.; Finklea, H. O.; Chidsey, C. E. D.; Linford, M. R.; Creager, S. E.; Ferraris, J. P.; Chalfant, K.; Zawodzinsk, T.; Feldberg, S. W.; Newton, M. D. *J. Am. Chem. Soc.* **2003**, *125* (7), 2004.
- (6) Richardson, J. N.; Peck, S. R.; Curtin, L. S.; Tender, L. M.; Terrill, R. H.; Carter, M. T.; Murray, R. W.; Rowe, G. K.; Creager, S. E. *J. Phys. Chem.* **1995**, *99*, 766.
- (7) Slowinski, K.; Slowinska, K. U.; Majda, M. *J. Phys. Chem. B* **1999**, *103*, 8544.
- (8) Bueno, P. R.; Mizzon, G.; Davis, J. J. *J. Phys. Chem. B* **2012**, *116* (30), 8822.
- (9) Gosavi, S.; Marcus, R. A. *J. Phys. Chem. B* **2000**, *104*, 2067.
- (10) Gosavi, S.; Gao, Y. Q.; Marcus, R. A. *J. Electroanal. Chem.* **2001**, *500*, 71.
- (11) Kim, J.; Kim, B. K.; Cho, S. K.; Bard, A. J. *J. Am. Chem. Soc.* **2014**, *136* (23), 8173.
- (12) Hill, C. M.; Kim, J.; Bard, A. J. *J. Am. Chem. Soc.* **2015**, *137* (35), 11321.
- (13) Kim, J.; Bard, A. J. *J. Am. Chem. Soc.* **2016**, *138* (3), 975.
- (14) Ahn, H. S.; Bard, A. J. *Angew. Chem.* **2015**, *127* (46), 13957.
- (15) Kavan, L.; O'Regan, B.; Kay, A.; Grätzel, M. *J. Electroanal. Chem.* **1993**, *346* (1–2), 291.
- (16) Eisenberg, D.; Ahn, H. S.; Bard, A. J. *J. Am. Chem. Soc.* **2014**, *136* (40), 14011.
- (17) Paracchino, A.; Laporte, V.; Sivula, K.; Grätzel, M.; Thimsen, E. *Nat. Mater.* **2011**, *10* (6), 456.
- (18) Paracchino, A.; Mathews, N.; Hisatomi, T.; Stefiik, M.; Tilley, S. D.; Grätzel, M. *Energy Environ. Sci.* **2012**, *5* (9), 8673.
- (19) Marcus, R. A. *J. Chem. Phys.* **1956**, *24* (5), 966.
- (20) Bard, A. J.; Faulkner, L. R. *Electrochemical Methods*, 2<sup>nd</sup> ed.; Wiley: New York, 2001.
- (21) Marcus, R. A. *J. Chem. Phys.* **1965**, *43* (2), 679.
- (22) Feldberg, S. W. *J. Electroanal. Chem. Interfacial Electrochem.* **1986**, *198* (1), 1.
- (23) Savéant, J. M.; Tessier, D. *J. Electroanal. Chem.* **1975**, *65* (1), 57.
- (24) Savéant, J.-M.; Tessier, D. *J. Phys. Chem.* **1977**, *81* (23), 2192.
- (25) Garreau, D.; Saveant, J. M.; Tessier, D. *J. Phys. Chem.* **1979**, *83* (23), 3003.
- (26) Corrigan, D.; Evans, D. H. *J. Electroanal. Chem. Interfacial Electrochem.* **1980**, *106*, 287.
- (27) Saveant, J.-M.; Tessier, D. *Faraday Discuss. Chem. Soc.* **1982**, *74*, 57.
- (28) Laborda, E.; Henstridge, M. C.; Compton, R. G. *J. Electroanal. Chem.* **2012**, *667*, 48.
- (29) Basame, S. B.; White, H. S. *Langmuir* **1999**, *15* (3), 819.
- (30) Kim, J.; Kim, B.-K.; Cho, S. K.; Bard, A. J. *J. Am. Chem. Soc.* **2014**, *136* (23), 8173.
- (31) Chazalviel, J. N.; Allongue, P. *J. Am. Chem. Soc.* **2011**, *133*, 762.
- (32) Zhao, J.; Bradbury, C. R.; Hudcova, S.; Potapova, I.; Carrara, M.; Fermín, D. J. *J. Phys. Chem. B* **2005**, *109* (48), 22985.
- (33) Bradbury, C. R.; Zhao, J.; Fermín, D. J. *J. Phys. Chem. C* **2008**, *112* (27), 10153.
- (34) Kissling, G. P.; Miles, D. O.; Fermín, D. J. *J. Phys. Chem. Chem. Phys.* **2011**, *13* (48), 21175.
- (35) Zhao, J.; Bradbury, C. R.; Fermín, D. J. *J. Phys. Chem. C* **2008**, *112* (17), 6832.
- (36) Dyne, J.; Lin, Y.-S.; Lai, L. M. H.; Ginges, J. Z.; Luais, E.; Peterson, J. R.; Goon, I. Y.; Amal, R.; Gooding, J. J. *ChemPhysChem* **2010**, *11* (13), 2807.
- (37) Liu, G.; Luais, E.; Gooding, J. J. *Langmuir* **2011**, *27* (7), 4176.
- (38) Shein, J. B.; Lai, L. M. H.; Eggers, P. K.; Paddon-Row, M. N.; Gooding, J. J. *Langmuir* **2009**, *25* (18), 11121.
- (39) Barfidokht, A.; Ciampi, S.; Luais, E.; Darwish, N.; Gooding, J. J. *Anal. Chem.* **2013**, *85* (2), 1073.
- (40) *CRC Handbook of Chemistry and Physics*, 89<sup>th</sup> ed.; Lide, D. R., Ed.; CRC Press: Boca Raton, FL, 2008.
- (41) Sung, Y.-E.; Gaillard, F.; Bard, A. J. *J. Phys. Chem. B* **1998**, *102* (49), 9797.
- (42) Breeze, A. J.; Schlesinger, Z.; Carter, S. A.; Brock, P. J. *Phys. Rev. B: Condens. Matter Mater. Phys.* **2001**, *64* (12), 125205.
- (43) Adriaanse, C.; Cheng, J.; Chau, V.; Sulpizi, M.; VandeVondele, J.; Sprik, M. *J. Phys. Chem. Lett.* **2012**, *3*, 3411.
- (44) Papaconstantopoulos, D. A. *Handbook of the Band Structure of Elemental Solids*, 2<sup>nd</sup> ed.; Springer: New York, 2015.
- (45) Bright, T. J.; Watjen, J. I.; Zhang, Z. M.; Muratore, C.; Voevodin, A. A.; Koukis, D. I.; Tanner, D. B.; Arenas, D. J. *J. Appl. Phys.* **2013**, *83515* (2013), 1.
- (46) Stassen, A. F.; De Boer, R. W. I.; Iosad, N. N.; Morpurgo, A. F. *Appl. Phys. Lett.* **2004**, *85* (17), 3899.
- (47) Tang, H.; Prasad, K.; Sanjines, R.; Schmid, P. E.; Levy, F. *J. Appl. Phys.* **1994**, *75* (4), 2042.
- (48) Stranks, D. R. *Discuss. Faraday Soc.* **1960**, *29*, 73.